Lab on a Chip

PAPER

View Article Online
View Journal | View Issue

Enabling practical surface acoustic wave nebulizer drug delivery via amplitude modulation

Cite this: *Lab Chip*, 2014, **14**, 1858

Anushi Rajapaksa,[a] Aisha Qi,[b] Leslie Y. Yeo,[b] Ross Coppel[c] and James R. Friend*[b]

Received 22nd February 2014,
Accepted 28th March 2014

DOI: 10.1039/c4lc00232f

www.rsc.org/loc

A practical, commercially viable microfluidic device relies upon the miniaturization and integration of all its components—including pumps, circuitry, and power supply—onto a chip-based platform. Surface acoustic waves (SAW) have become popular in microfluidic manipulation, in solving the problems of microfluidic manipulation, but practical applications employing SAW still require more power than available via a battery. Introducing amplitude modulation at 0.5–40 kHz in SAW nebulization, which requires the highest energy input levels of all known SAW microfluidic processes, halves the power required to 1.5 W even while including the power in the sidebands, suitable for small lithium ion batteries, and maintains the nebulization rate, size, and size distributions vital to drug inhalation therapeutics. This simple yet effective means to enable an integrated SAW microfluidics device for nebulization exploits the relatively slow hydrodynamics and is furthermore shown to deliver shear-sensitive biomolecules—plasmid DNA and antibodies as exemplars of future pulmonary gene and vaccination therapies—undamaged in the nebulized mist. Altogether, the approach demonstrates a means to offer truly micro-scale microfluidics devices in a handheld, battery powered SAW nebulization device.

1 Introduction

The average cost of developing a drug is currently just over USD800 million. This enormous cost and the nine to fourteen years required to bring a drug to market, just barely in time before patent expiration,[1] are the reasons drugs are both expensive and targeted at lucrative markets. Beyond the extraordinary costs to the public healthcare system, pharmaceutical companies will naturally only pursue drugs that offer a decent return on investment. Pulmonary system-delivered drugs have the longest development times and are the most expensive of all, at over USD1 billion per drug, because delivery to the lung is notoriously fraught with problems. Pulmonary drug delivery of dry particle formulations require extensive development to formulate stable dry particles that avoid lung damage in the long run,[2] and yet over 50% of patients are unable to properly nor reliably use delivery devices to inhale such drugs into the lungs,[3] a long-standing problem that remains today.[4,5]

Among the few drugs to survive development and achieve commercial success via pulmonary delivery have been dry particle formulations for the treatment of asthma and chronic obstructive pulmonary disease, delivered by modern pressurized metered dose inhalers and dry powder inhalers that are nearly identical to the original push-and-breathe concept introduced in the 1950s.[6] An especially promising advance was the development of technology that synchronizes delivery of the aerosol to the patient's breathing to reduce the amount of drug waste,[7] though its requirement of a combination of built-in sensors, electronic control schemes, and active aerosol generation mechanisms has prevented its wider adoption, and the cost issue in developing a dry particle formulation remains. Recent adaptations of integrated-circuit fabrication techniques to microfluidics promise to address these issues, but the remaining requirement of a large and complex power supply and ancillary equipment required to drive such devices leaves them impractical for their intended application: personal, daily use by a patient.

Nebulizers represent a potential alternative by delivering liquid droplet mists, but are large, inconvenient, and rapidly degrade most biomolecules.[8] They are preferred for the treatment of patients not trained to use inhalers[9] and only require the drug to be dissolved in a carrier in formulations similar to those required for syringe injection. Certainly there are other methods of drug delivery, but these have their own problems. Pills are convenient, yet require the drug to survive the gastrointestinal tract without damage,[10] a distinct challenge. Injections are uncomfortable, relatively expensive when considering the drug to be delivered, unsuitable in unsanitary

[a] *Micro/Nanophysics Research Laboratory, Monash University, Clayton, VIC 3800 Australia*
[b] *Micro/Nanophysics Research Laboratory, RMIT University and the Melbourne Centre for Nanofabrication, Melbourne, VIC 3001 Australia. E-mail: james.friend@rmit.edu.au; Tel: +61 (0)3 9925 0465*
[c] *Department of Microbiology, Monash University, Clayton, VIC 3800, Australia*

conditions, and require expertise in proper delivery.[11] Finally, new drug delivery transdermal patches currently accommodate only small molecular weight drugs.[12]

Vaccination, gene therapy and the treatment of other diseases such as cystic fibrosis and lung cancer all represent potential therapeutic applications of a personal nebulizer given the suitability of pulmonary drug administration for efficient, reproducible, non-invasive, safe and low-cost systemic delivery of certain peptides, proteins and pDNA.[13,14] Effective disease treatment and vaccination options in disadvantaged areas of the world are nearly absent; the pulmonary route represents one of the few ways to deliver medications without likewise increasing the risk of infection and cross-contamination of disease due to needle sharing and unsanitary conditions. An inexpensive pulmonary delivery system would represent a potential solution to this problem.

2 Concept

Though the original SAW microfluidic aerosol delivery platform[15,16] was driven by a palm-sized battery-powered circuit (Fig. 1), the limited power output available from the circuit imposed an unacceptable constraint on the aerosol production rate that prevents practical use of the technology in delivering drugs over one or a few inhalations. Increasing the power available to the device requires the use of larger driver circuits (Fig. 1(b)) that prohibit a complete miniaturized package for portable use. Such packages would furthermore be useful for a broader collection of applications, and is especially useful now that there is a rapidly expanding interest in the technology to deliver microdevices for biomedical applications via acoustic microfluidics.[17–20]

A modest power reduction of one-third through the use of a metallic horn and waveguide pattern placed in front of the interdigital transducer electrodes (IDTs) used to generate the SAW has been demonstrated,[21] though the nebulization rate was modest at approximately 50 μl min^{-1}. Another simple yet effective means of improving power efficiency in SAW devices has been shown using pulse width modulation (1 kHz) of the input signal (into a crude 9.8 MHz device for nebulization);[22] though an incredible nebulization rate of 600 μl min^{-1} was achieved, extremely high voltages were necessary, as high as 180 V_{p-p}, and the aerosol size distribution was very polydisperse, spanning a size range from sub-micron to nearly one millimeter. Using modulation to overcome the pinning forces present in sessile drops for digital microfluidics has been examined as well,[23] though a necessary assessment of the effects of such modulation on chemicals and biological materials has not yet been performed for any application.

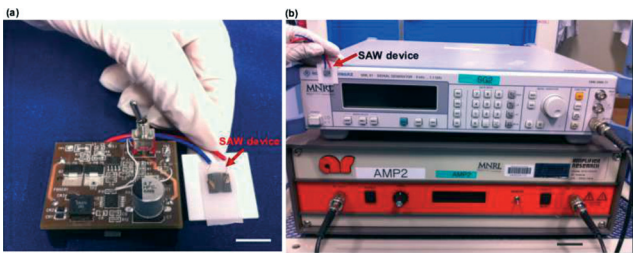

Fig. 1 (a) Initial prototype of the battery-powered circuit to be used to drive the SAW microfluidic aerosol delivery platform (scale bar = 1 cm). (b) Typical signal generator and amplifier used in laboratory settings to provide sufficient power for SAW nebulization (scale bar = 3 cm).

Here, we propose an amplitude modulation scheme for further reducing the power requirements to allow battery-powered operation from a similar driver circuit but also increases the aerosol delivery rate. Amplitude modulation was the original method for radio transmission,[24] and long used in a variety of related disciplines where the sinusoidal radio-frequency carrier signal is modulated by an audio-frequency signal before transmission.[25] The power of the transmitted signal is carried at both the carrier frequency, or in this study the SAW frequency, f, and the sidebands present at $f - f_{mod}$ and $f + f_{mod}$. If the modulation is 100% as it is in this study, implying that the amplitude is reduced to zero twice for each period of oscillation of the modulation signal, the total power present in the sidebands is one-half the power carried at the carrier frequency. Over the years, more complex amplitude modulation schemes have been devised[26] to control the power distribution, allocating it to the sidebands (DSB) or only one of the two sidebands (SSB), but here we report only the total power transmitted by the modulated signal, the power in the sidebands and the carrier signal, as this is what is most important in determining the device's power usage.

Because nebulization as a hydrodynamic phenomena is relatively slow in comparison to the SAW, amplitude modulation at relatively low frequencies is likely possible without upsetting the hydrodynamics—but must be confirmed because the coupling mechanisms are strongly nonlinear. This idea goes further: the modulation itself may aid the nebulization, driving it directly and potentially more efficiently, if the modulation frequency matches the excitation frequency of the capillary-viscous mechanism responsible for the nebulization.[27] Though the frequency of the SAW that induces nebulization here is 10–100 MHz order, the actual droplet formation mechanism occurs at a remarkably low 10 kHz order frequency by comparison. The SAW induces a turbulent jet in the fluid meniscus present on the substrate surface that drives broadband excitation of capillary waves on the free surface in a complex process[28] that leads to nebulization by a capillary-viscous mechanism at a frequency determined by[27,29]

$$f \sim \frac{\gamma}{\mu R}, \quad (1)$$

implying that a parent drop with a characteristic dimension $R \sim 10^{-3}$ m comprising typical fluids with surface tension $\gamma \sim 10^{-2}$ kg s^{-2} and viscosity $\mu \sim 10^{-2}$–10^{-3} kg (m s)$^{-1}$ typically vibrates under resonance at 1–10 kHz-order frequencies.

Given the intent to use this technology for pulmonary gene and vaccine delivery, DNA and antibodies are used during the nebulization process as exemplars of typical biomolecules

that might be used with the system. One of the common concerns of relatively low frequency (audible to ultrasonic) excitation is the damage to large molecules in the fluid to be nebulized.[30] This is caused by large shear stresses exerted on the molecule either by the hydrodynamics or cavitation. The modulation of the SAW is to be conducted in this frequency range, and so a significant portion of our study reported below is devoted to the investigation of the continued viability of large biomolecules after nebulization. In past work, proteins, polymers, and even cells have been shown to remain intact through the SAW nebulization process,[16,31,32] and the aerosol drop size distribution has been shown to be within the optimum respirable size range (1–10 μm) necessary for oropharyngeal and deep lung delivery.[33–35] Introducing amplitude modulation, however, particularly in the frequency range where molecular damage has been reported in the past,[30] may give entirely different results than with continuous SAW alone. Therefore, its effects on the drop distribution and the condition of the molecules after nebulization must be examined.

While we demonstrate the use of amplitude modulation here for reducing the power requirements in SAW nebulization devices, the same scheme can be applied to the entire range of SAW microfluidics for miniaturization toward true lab-on-a-chip functionality. A review of SAW microfluidic devices is given elsewhere[17,36] and a myriad of SAW devices have been proposed for applications ranging from fluid manipulation, *e.g.*, droplet transport,[37,38] microchannel pumping,[39–41] mixing[42,43] and jetting,[44] particle sorting and concentration[43,45] to chip-scale chemical and biochemical synthesis,[46,47] biosensing,[48] and microfluidic chip interfacing with mass spectrometry;[49,50] in addition, it is also possible to exploit SAW to drive these microfluidic manipulations on disposable superstrates.[51,52]

3 Experiments and materials

The 30 MHz SAW device employed in our experiment, illustrated in Fig. 2, consisted of a low-loss piezoelectric material, 127.86° *Y*-rotated, *X*-propagating single-crystal lithium niobate (LN), upon which were fabricated a pair of single-phase unidirectional transducers (SPUDT) via standard UV photolithography processes in 5 nm Cr under 250 nm Al. The width and gap of the interlaced finger patterns of the SPUDT determines the SAW wavelength λ_{SAW}; in this study, λ_{SAW} = 132 μm corresponds to a SAW and carrier frequency of 30 MHz. The curved SPUDTs focus the acoustic energy to which fluid is delivered from a reservoir via a pre-wetted paper wick embedded at the tip of a capillary tube[16] that allows continuous flow of fluid without the need of a syringe pump. As a sinusoidal electrical input at the SAW frequency (convolved with amplitude modulation where appropriate) is applied to the SPUDT, SAWs are generated that propagate along the LN substrate across to the leading edge of the paper wick, where they continuously draw liquid out from the paper onto the substrate to form a thin film.[16] Since acoustic energy also leaks into the liquid film, the free surface of the film destabilizes and, beyond a critical input power, breaks up to form aerosol droplets (Fig.2(d)).[29] There is no observable flow onto the device in the absence of SAW (for example, that might which be present due to evaporation), and hence the flow rate through the capillary tube, measured using the graduated scale marked on the tube, is a good estimate of the

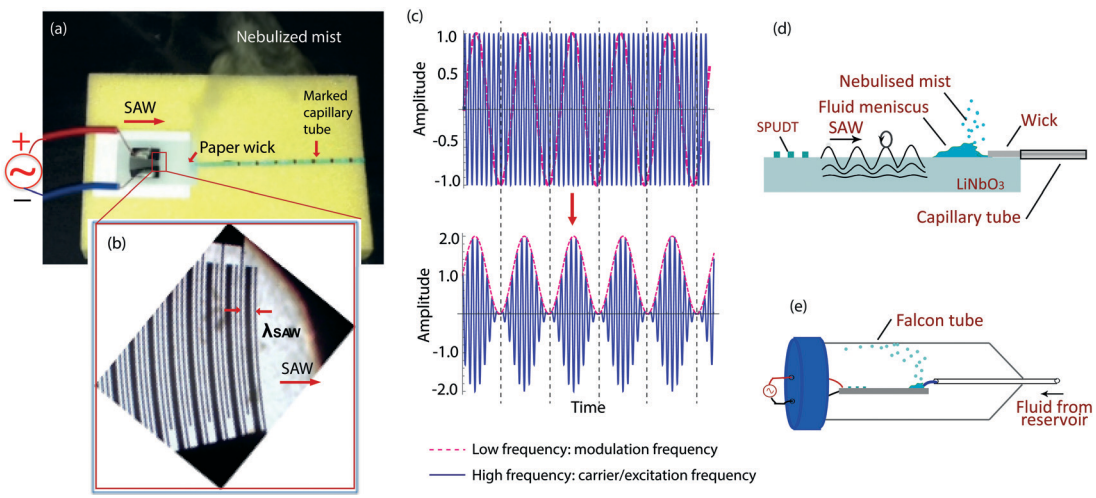

Fig. 2 (a) Image of a 30 MHz SPUDT SAW device. The fluid is delivered to the SAW substrate through a paper strip embedded in a capillary tube which is connected to a reservoir. In order to record the aerosol production rate, the capillary tube was marked along its length at 0.5 cm intervals. (b) Enlarged view of the SPUDT. The width and gap of the interleaved finger electrodes determine the SAW wavelength λ_{SAW}, 132 μm for a 30 MHz device, defining the (c) high-frequency, carrier wave that is modulated at a lower frequency for power savings. (d) A schematic illustration of the SAW nebulization mechanism. The SAW (not shown to scale) propagates along the substrate and leaks energy into the liquid film to nebulize the meniscus that forms adjacent a paper wick providing the fluid to the substrate from a capillary tube connected to a reservoir.[15] Collection of the aerosolized DNA or antibodies is accomplished by (e) placing the device within a conical Falcon™ tube (50 ml, BD Biosciences, San Jose, CA) for further *in vitro* characterization of their post-nebulization viability.

aerosol production rate given that the film dimensions can be assumed to be fairly constant during nebulization.

To study the effect of amplitude modulation on SAW nebulization, the following set of experiments were performed:

The effect of amplitude modulation on the aerosol size of deionized water droplets generated via SAW nebulization were quantified by a single aerosol size parameter D_{v50}, representing the mean diameter across the 50th percentile within the volume size distribution and measured using laser diffraction (Spraytec, Malvern Instruments, Malvern, UK).

The effect of amplitude modulation on the nebulization rate of deionized water as a model fluid was determined by filling the capillary tube (without the reservoir) and completely wetting the paper wick. As the water was nebulized, the time was recorded as the meniscus retracted past each graduation on the capillary tube shown in Fig. 2(a). Experiments were repeated three times at each sinusoidal amplitude modulation frequency: 500 Hz, 1 kHz, 5 kHz, 10 kHz, 20 kHz, and 40 kHz. Since amplitude modulation results in the onset of nebulization at lower (total: carrier and sideband) power levels, these levels (1.5 and 2 W) were used to assess the device's performance. Control experiments were carried out in the absence of amplitude modulation where power levels of 1.5, 2, 3 and 4 W were used.

Amplitude modulation's effect on plasmid DNA delivery was assessed through preparation of plasmid DNA containing an influenza A virus surface antigen, human haemagglutinin (A/Solomon Islands/3/2006 (egg passage) (H1N1) strain), cloned into the mammalian expression vector VR1020 (Vical Inc., San Diego, CA) (Fig. 3). The entire coding sequence of HA was amplified by polymerase chain reaction using primers forward and reverse that incorporated a BamHI site at the 5° end and a EcoRI site at the 3° end. Forward: 5°-CGCGGATCCATGAAAGTAAAACTACTGGTCCTGTTATG-3°; reverse: 5°-CCGGAATTCTTGTTTGTAATCCCAT-TAATGGCATTTTGT-3°. The PCR product was digested with BamHI/EcoRI and ligated into the 3 °C plasmid, VR1020, resulting in plasmid VR1020–HA. A colony of *E. coli* DH5α transformed with the plasmid VR1020–HA (~6 kbp) was picked from a streaked selective plate and inoculated in 10 ml of LB medium containing 100.0 g ml^{-1} of kanamycin. The starter culture was incubated at 37 °C and agitated at 200 rpm for 8 h before being transferred to five separated 200 ml LB media, and further cultured for 12 h. The cell cultures were stored at −70 °C for subsequent use. The plasmids were purified from cells using an endotoxin-free plasmid purification kit (Plasmid Mega Kit, QIAGEN Pty. Ltd., Doncaster, VIC, Australia) according to the manufacturer's instructions. Nebulization was confined in a 50 ml conical Falcon tube (BD Bioscience, Franklin Lakes, NJ), as depicted in Fig. 2(e). Plasmid DNA aerosols were collected after condensation on the Falcon tube wall. Both control and nebulized pDNA samples were analysed for potential alterations in the plasmid structure with 1% agarose gel electrophoresis that used GelRed™ staining, and a 1 kbp DNA ladder was employed as a size marker. The gel was made up of 5 g agarose at 1× dilution of TAE buffer (242.0 g Tris base, 57.1 ml CH_3COOH, 9.3 g of EDTA). The electrophoresis was carried out at 120 VDC for 60 min. The resulting gel was analysed and imaged in an automated gel imaging system (Molecular Imager® Gel Doc XR, Bio-Rad Laboratories Inc., Hercules, CA). The intensity of the bands for each structure corresponds to the number of DNA molecules. The percentage of supercoiled (sc) and open circular (oc) to fragmented DNA was quantified via densitometry software (Quantity One®, Bio-Rad Laboratories Inc., Hercules, CA) by comparing pre- and post-nebulized samples.

The effect of amplitude modulation on protein delivery was performed using rabbit anti-YFP (yellow fluorescence protein) antiserum solution (diluted at 1 : 20) obtained from collaborators at the Coppel Lab (Department of Microbiology, Monash University) and used in the same manner as that for the pDNA. The antibody was then detected using dot blot analysis where 5 μl of YFP protein solution was dotted onto a transfer membrane (PolyScreen® PVDF, PerkinElmer Inc., Waltham, MA) for immunoblotting. The membranes were incubated in TBS-T buffer (0.05 M Tris-HCl pH 7.4, 0.15 M NaCl, 0.05% Tween 20) containing 5% non-fat milk powder overnight at 4 °C. Subsequently, the membranes were probed with nebulized anti-YFP antiserum solutions for 1 h at room temperature, and washed three times in TBS-T for 10 min each time. Primary antibody reactivity to immunoblotted proteins was detected with anti-rabbit immunoglobulin conjugated to horseradish peroxidase (HRP; Silenus Laboratories Pty. Ltd., Hawthorn, VIC, Australia) and visualized by Renaissance® Western Blot Chemiluminescence Reagent (NEN Life Science, PerkinElmer Inc., Waltham, MA).

Statistical analysis for the entire study was performed using SPSS (statistics 19, IBM Corporation, Armonk, NY USA) to accommodate normally and non-normally distributed results. One-way ANOVA with Tukey's post-hoc test was used for data that survived Levene's test of equality of error variances; in other words when the null hypothesis of equal variances between the data sets is judged to be valid with significance $p \geq 0.05$, suggesting the data is normally distributed and

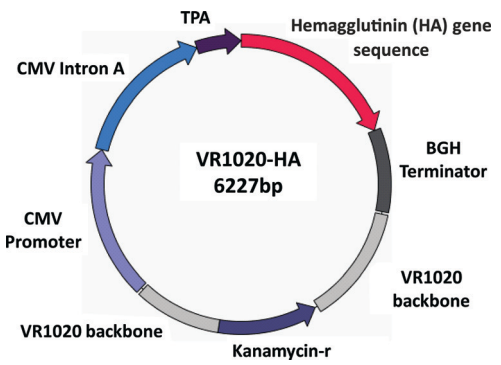

Fig. 3 Representation of pVR1020 with vector encoding the haemagglutinin (HA) gene sequence. The gene encoding HA is inserted in a plasmid, VR1020, that contains a secretion signal of tissue plasminogen activator (TPA), human cytomegalovirus (CMV) early promoter, CMV intron A, bovine growth hormone (BGH) terminator, and kanamycin resistance gene.

therefore ANOVA was suitable. In instances where the Levene's test of equality of error variances was significant ($p < 0.05$), the non-parametric Kruskal–Wallis test was used instead to test for significance. All data are expressed as the mean ± standard deviation. The results were considered significant if $p < 0.05$.

4. Results and discussion

4.1 Production rate and aerosol size

Table 1 shows the nebulization rate at each power level, with and without application of amplitude modulation. The rate at which aerosols are produced at 1.5 and 2 W is roughly quadrupled and trebled, respectively, when amplitude modulation is employed. Taken a different way, the power required to achieve satisfactory aerosol delivery for a portable handheld nebulization device, typically 100 μl min^{-1} or more, is halved with the use of the amplitude modulation scheme. If one is concerned with the operating lifetime of the device on a battery, for example, choosing to operate the system at 1.5 W continuously without amplitude modulation on a small Li ion camera battery (NB–6L, 1000 mAh at 3.7 V, Canon, Utsunomiya, Japan), and presuming only 50% of the energy is available to the nebulizer, the remainder used up in the circuit, perhaps, then the nebulizer would operate for about 1.2 hours, nebulizing 1.7 ml of fluid before the battery discharges. However, operating continuously with amplitude modulation at 0.5 kHz, it would produce 7.6 ml of fluid over the same time. Operating occasionally to deliver the same amount of fluid, 1.7 ml, the nebulizer's battery would last 5.4 hours with amplitude modulation.

From Table 1, we note that the nebulization rate is slightly reduced as the amplitude modulation frequency is increased, particularly beyond 10 kHz and beyond the capillary-viscous resonant frequency of 10 kHz order (as estimated from eqn (1)). Curiously, it appears that to drive superior nebulization, amplitude modulation to drive direct coupling into the capillary wave is better when at a frequency nearer the fundamental resonance of the fluid meniscus on the substrate, on the order of 100 Hz. This is likely due to superior coupling between the acoustic pressure-mediated excitation and oscillation of the fluid's free surface at the drop's fundamental resonance compared to higher frequencies, and the presence of a period-halving cascade in the capillary wave system that strongly couples energy upwards in frequency at a rate $f^{-15/6}$.[28]

When comparing the optimal aerosol production rate to the results obtained with past SAW nebulizers, employing pulse width modulation (1 kHz) of the input signal for a SAW device at 9.8 MHz,[22] voltages of around 120–140 V_{p-p} were required to achieve production rates of 200 μl min^{-1}. For the SAW devices in the current study without amplitude modulation, voltages of around 50 V_{p-p} are required to achieve similar aerosol production rates, an improvement in part due to an improved IDT design by having an appropriate number of finger pairs to improve impedance matching with the source, to an increase in frequency to 30 MHz to avoid parasitic losses of the SAW which extends through the wafer thickness all the way to the bottom face for a 500 μm-thick LN wafer at 9.8 MHz, and in part due to improved IDT fabrication techniques that produce lower electrode resistance. Employing amplitude modulation substantially reduces the required voltage to as little as 35 V_{p-p}. These voltage decreases are not directly indicative of an improvement in performance, as the current may increase to compensate as happens when the frequency of operation is increased while holding other aspects of the design constant. However, they are practically beneficial when designing appropriate handheld driver circuits. Table 2 is a compilation of measured aerosol sizes showing the effect of amplitude modulation and the effect of the amplitude modulation frequency.

We have examined the nebulization phenomena at length as reported in a number of papers,[15,27] and, in particular, found[29] that for the configuration used in this study with a

Table 1 Effect of amplitude modulation at various frequencies on the nebulization rate

Input power (W)	No ampl. mod. rate (μl min^{-1})	Amplitude modulation	
		Freq. (kHz)	Rate (μl min^{-1})
1.5	23.4 ± 2.1	0.5	103.7 ± 14.2
		1	85.1 ± 16.3
		5	80.5 ± 9.4
		10	43.2 ± 4.3
		20	56.6 ± 6.3
		40	50.4 ± 5.9
2	50.8 ± 2.2	0.5	126.8 ± 22.8
		1	103.8 ± 13.5
		5	100.3 ± 11.5
		10	111.4 ± 13.3
		20	77.0 ± 8.0
		40	74.9 ± 6.4
3	134.9 ± 15.2		
4	211.9 ± 71.1		

Table 2 Effect of amplitude modulation at various frequencies on the aerosol volume mean diameter D_{v50}. For each experiment, the fluid was nebulized for 20 seconds with 50 data points sampled every second. This was repeated four times for every parameter set, *i.e.*, n = 4000 data points for each set of parameter values

Input power (W)	No amplitude mod. D_{v50} (μm)	Amplitude modulation	
		Freq. (kHz)	D_{v50} (μm)
1.5	7.29 ± 0.90	0.5	9.75 ± 1.89
		1	8.55 ± 0.72
		5	7.94 ± 0.08
		10	8.63 ± 0.89
		20	8.32 ± 0.15
		40	7.76 ± 0.21
2	8.53 ± 1.06	0.5	9.69 ± 1.38
		1	11.25 ± 0.61
		5	9.15 ± 0.53
		10	9.01 ± 1.36
		20	8.13 ± 0.10
		40	7.80 ± 0.34
3	10.51 ± 1.09		
4	10.18 ± 0.70		

paper wick providing the fluid for nebulization and furthermore defining the meniscus geometry,

$$D \sim \frac{\gamma H^2}{\mu L^2} \frac{\mathrm{We}^{2/3}}{f}, \quad (2)$$

where H and L are characteristic height and length scales of the liquid drop or film, and $\mathrm{We} = \rho L(u_0)^2/\varepsilon\gamma$ is an acoustic Weber number where u_0 is the vibration velocity of the SAW substrate, implying that We ~ P where $P \sim \rho u_0{}^2$ represents the input acoustic power into the drop. Therefore, the droplet diameter produced by the nebulizer $D \sim P^{2/3}$, consistent with the result in Table 2, where a significant (Tukey's post hoc test) increase in aerosol size from the low 1.5 W input to higher power levels of 3 W ($p = 0.061$) and 4 W ($p = 0.028$) was seen.

Importantly, other than the increase in the aerosol size with the application of amplitude modulation at the specific case of 1 kHz at 2 W ($p = 0.03$), there was no significant change in the nebulization due to amplitude modulation at both 2 W (Tukey's post hoc test) and 1.5 W (Kruskal–Wallis Test). Since the capillary wave response frequency spectrum is known to be independent of the excitation frequency in a sessile drop,[28] the result here, with the meniscus geometry and the associated aspect ratio H/L largely defined by the wick, is not a surprise. In any case, the absence of any significant change in the aerosol size with amplitude modulation of the SAW signal is helpful in practical application of the technology in pulmonary delivery, as the aerosol diameters need to lie in the 1–10 μm range for optimal deposition in the oropharyngeal and lower respiratory tract region.

4.2 Post-nebulization biomolecular integrity and viability

Besides the physical dimensions of the droplets generated during nebulization, the intended application of the technology in drug delivery requires an assessment of the molecular damage incurred through nebulization. Cells and proteins in suspension have been shown to tolerate, with little damage, 10–100 MHz order SAW up to a few watts of input power with arrangements similar to the one in this study and typical of nebulization.[16,31,53] This was primarily attributed to the absence of cavitation in SAW irradiation at these powers, but is also due to the short time scales of the 10–100 MHz order oscillating signal, several orders of magnitude smaller than the characteristic hydrodynamic time scale responsible for molecular or cellular damage through shear.[27] Here, we carry out a brief study employing two large model molecules, plasmid DNA (pVR1020–HA) and an antibody (rabbit anti-YFP antisera), to span the spectrum of potential applications for the SAW inhalation therapy platform across gene and vaccine delivery. Consistent with past results, 80% of supercoiled pDNA, for example, remains intact after nebulization in the absence of amplitude modulation (Fig. 4).

However, introducing low-frequency amplitude modulation may strongly affect the integrity of the molecules and cells, particularly when the modulation is between 20 and 50 kHz—the very frequencies used in acoustic sonoporation

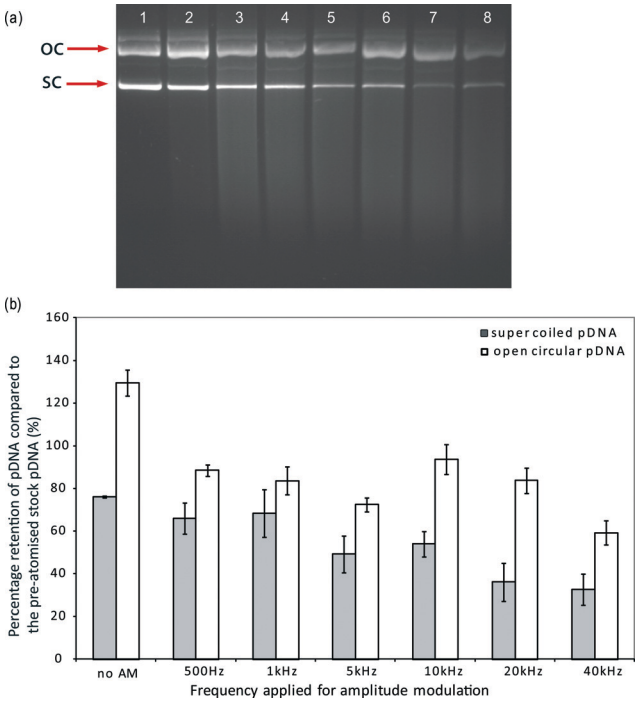

Fig. 4 (a) Gel electrophoresis of post-nebulized plasmid DNA showing the effect of the amplitude modulation at various frequencies on the structural integrity of the pDNA. Lane 1: control pDNA sample without SAW exposure; lane 2: nebulization at 1.5 W without amplitude modulation; lanes 3–8: nebulization at 1.5 W with amplitude modulation at 500 Hz, 1 kHz, 5 kHz, 10 kHz, 20 kHz and 40 kHz, respectively. Each lane was loaded with 250 ng pDNA and representative gels from three independent experiments are shown. Arrows indicate the position of the open circular (OC) and supercoiled (SC) forms of the pDNA. (b) Percentage retention of post-nebulized supercoiled (shaded) and open circular (unshaded) pDNA compared to the unnebulized sample. The results shown are the mean of triplicate nebulization runs.

of cells and molecular scission via hydrodynamic shear and cavitation.[8,54,55] For example, plasmid DNA fragmentation occurs under typical strain rates of 10^{-5}–10^{-6} s^{-1}, corresponding to oscillations in the 100 kHz to 1 MHz range. Though this is fortuitously between the 10–100 MHz order SAW carrier and the 1–10 kHz order modulation frequencies used in this study, the true range of strain rates that lead to pDNA damage is unclear.[56]

4.2.1 Plasmid DNA. Turning on amplitude modulation at 500 Hz, the retained supercoiled pDNA fraction remains roughly equivalent to the modulation-free results, gradually decreasing to around 50% as the modulation frequency is increased to 10 kHz, only to sharply drop to 30% as the carrier frequency is increased further to 40 kHz. This transition is closer to the 100 kHz order frequencies reported to produce sufficient shear rates to induce uncoiling and damage of the pDNA, and is consistent with the typical 20–50 kHz frequency range used in sonoporation and scission. A reasonable rationale in selecting amplitude modulation frequencies during nebulization is therefore to choose lower frequencies, at 1 kHz for example, to minimize pDNA denaturation and, as it happens, improve the nebulization performance.

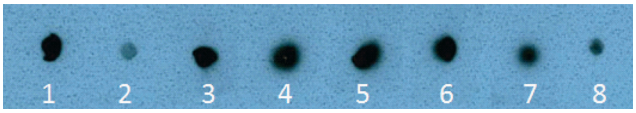

Fig. 5 Post-nebulized YFP antibody samples spotted onto a dot blot showing the preservation of the bioactivity of protein molecules in samples with and without amplitude modulation. Lane 1: no nebulization; lane 2: nebulization at 1.5 W in the absence of amplitude modulation; lanes 3–8: nebulization at 1.5 W with amplitude modulation at frequencies of 500 Hz, 1 kHz, 5 kHz, 10 kHz, 20 kHz and 40 kHz, respectively.

The effect of the amplitude modulation on the amount of open circular pDNA is more complex. Without amplitude modulation, the concentration of open circular pDNA is >100%, indicating that in addition to the open circular pDNA present in the original feedstock, much of the supercoiled pDNA that was scissioned became open circular pDNA rather than linear chains or fragments. Since open circular pDNA is still biologically functional, this is an attractive result that does not completely extend to the amplitude modulation results. With amplitude modulation, the open circular pDNA was roughly 90%, indicating that as the frequency of modulation increased, the damage to the supercoiled pDNA produced roughly the same amount of open circular pDNA. While this is a 40% drop from the modulation-free case, the concentration of open circular pDNA in the original sample is very low to begin with, which can substantially exaggerate the apparent effects of modulation on the open circular pDNA concentration percentages, and is not a reason to choose one amplitude modulation scheme over another. At the highest modulation frequencies, the relatively low percentages of supercoiled pDNA together with the decreasing open circular pDNA fraction together suggest the scission of the pDNA is far more thorough.

4.2.2 Antibodies. Antibodies, like pDNA, are fragile and sensitive to hydrodynamic shear, but the bioactivity of an exemplar antibody to YFP is not significantly affected across the range of amplitude modulation frequencies used in this study by amplitude-modulated SAW according to a dot blot test. Composed of proteins, the YFP antibodies' post-nebulized bioactivity serves to indicate how the general class of protein-based molecules will tolerate pulmonary administration using the SAW nebulizer. Due to the small quantities of antibody present in the post-nebulized samples, it is not possible to obtain quantitative measurements of the post-nebulized antibody bioactivity; nevertheless, the qualitative results from the dot blot test in which YFP was spotted using post-nebulized rabbit anti-YFP antisera (Fig. 5) is of sufficient fidelity to confirm the antibody remains functional with or without amplitude modulation.

5 Conclusions

We have demonstrated the feasibility of applying amplitude modulation in halving the required power while maintaining the aerosol production rate of SAW nebulization—an important consideration that addresses current issues hindering the miniaturization and integration of the power supply into a practical and commercially realisable portable handheld nebulizer platform for the pulmonary administration of a wide variety of therapeutic targets. Taken another way, at 1.5 W input power, the amplitude modulation-driven nebulization occurred at a rate three times the continuously driven version, making any such use of this technology three times quicker for a patient. We verified that the introduction of amplitude modulation in the system does not significantly alter the aerosol droplet diameter from the respirable size range for optimal dose administration to the oropharyngeal and lower respiratory tract. Judiciously limiting the amplitude modulation carrier frequency to 1 kHz simultaneously optimises the nebulization rate while limiting loss of bioactivity through pDNA fragmentation as well as protein denaturation, both of which represent important therapeutic targets for gene and vaccine delivery. These results therefore lend confidence to the attractiveness and feasibility of the SAW nebulization platform as a true miniaturized and integrated handheld platform for portable inhalation therapy from a practical and commercial standpoint for applications as ubiquitous as asthma and chronic obstructive pulmonary diseases to exciting future possibilities in non-invasive gene and vaccine administration to treat a variety of diseases. In addition, the results of the study can also be extrapolated to reduce the power requirements and hence afford the miniaturization and integration of the power supply with the existing chip-based SAW microfluidic platform to drive a whole range of microscale and nanoscale fluid actuation and bioparticle manipulation processes on a truly integrated chip-scale device.

Acknowledgements

This work was supported by funding provided through the Walter Jona Grant for Paediatric Asthma Research awarded by the Asthma Foundation Victoria. LYY is supported by an Australian Research Fellowship awarded by the Australian Research Council through Discovery Project DP0985253. Some of this work was conducted at the Melbourne Centre for Nanofabrication (MCN). JRF is grateful to the Australian Research Council for grants DP120100013 and DP120100835 in support of this work, and appreciates the Melbourne Centre for Nanofabrication's contribution through his Senior Tech Fellowship and RMIT University for his Vice-Chancellor's Senior Research Fellowship. The authors acknowledge the kind assistance of Charles Ma, Kartika Setyabudi, Ming Tan, and Peggy P. Y. Chan in this work.

References

1 C. P. Adams and V. V. Brantner, *Health Affairs*, 2006, **25**, 420–428.
2 J. Kling, *Nat. Biotechnol.*, 2008, **26**, 479–480.
3 G. Crompton, *Lung*, 1990, **168**, 658–662.
4 D. E. Geller, *Respir. Care*, 2005, **50**, 1313–1322.

5 A. S. Melani, M. Bonavia, V. Cilenti, C. Cinti, M. Lodi, P. Martucci, M. Serra, N. Scichilone, P. Sestini and M. Aliani, *et al.*, *Respiratory Medicine*, 2011, **105**, 930–938.
6 L. Y. Yeo, J. R. Friend, M. P. McIntosh, E. Meeusen and D. Morton, *Expert Opin. Drug Delivery*, 2010, **7**, 663–679.
7 J. Denyer, K. Nikander and N. Smith, *Expert Opin. Drug Delivery*, 2004, **1**, 1656–1676.
8 E. R. Arulmuthu, D. J. Williams, H. Baldascini, H. K. Versteeg and M. Hoare, *Biotechnol. Bioeng.*, 2007, **98**, 939–95.
9 A. Hickey, *Pharmaceutical inhalation aerosol technology*, Marcel Dekker, 2nd edn, 2004.
10 A. Florence and P. Jani, *Drug Saf.*, 1994, **10**, 233.
11 Y. Hutin and R. Chen, *Bull. W. H. O.*, 1999, **77**, 787.
12 M. R. Prausnitz and R. Langer, *Nat. Biotechnol.*, 2008, **26**, 1261–1268.
13 B. L. Laube, *Respir. Care*, 2005, **50**, 1161–1176.
14 D. Lu and A. Hickey, *Expert Rev. Vaccines*, 2007, **6**, 213–226.
15 A. Qi, J. R. Friend and L. Y. Yeo, *Lab Chip*, 2009, **9**, 2184–2193.
16 A. Qi, L. Yeo, J. Friend and J. Ho, *Lab Chip*, 2010, **10**, 470–476.
17 J. Friend and L. Y. Yeo, *Rev. Mod. Phys.*, 2011, **83**, 647–704.
18 T.-D. Luong and N.-T. Nguyen, *Micro Nanosyst.*, 2010, **2**, 217–225.
19 S.-C. S. Lin, X. Mao and T. J. Huang, *Lab Chip*, 2012, **12**, 2766–2770.
20 L. Y. Yeo and J. R. Friend, *Annu. Rev. Fluid Mech.*, 2013, **46**, 56006.
21 W. Soluch and T. Wrobel, *Electron. Lett.*, 2006, **42**, 1432.
22 K. Nagase, J. Friend, T. Ishii, K. Nakamura and S. Ueha, *Proceedings of the 22nd Symposium on Ultrasonic Electronics*, Ebina, Japan, 2001, pp. 377–378 (in Japanese).
23 M. Baudoin, P. Brunet, O. Bou Matar and E. Herth, *Appl. Phys. Lett.*, 2012, **100**, 154102–154102.
24 R. A. Fessenden, *Trans. Am. Inst. Electr. Eng.*, 1908, **27**, 553–629.
25 M. Filipovic, *Radio Receivers*, mikroElektronika, 2007.
26 R. Gallager, *Principles of Digital Communication*, Cambridge University Press, 2008.
27 A. Qi, L. Yeo and J. Friend, *Phys. Fluids*, 2008, **20**, 074103.
28 J. Blamey, L. Y. Yeo and J. R. Friend, *Langmuir*, 2013, **29**, 3835–3845.
29 D. J. Collins, O. Manor, A. Winkler, H. Schmidt, J. Friend and L. Yeo, *Phys. Rev. E: Stat., Nonlinear, Soft Matter Phys.*, 2012, **86**, 056312.
30 Y. Lentz, T. Anchordoquy and C. Lengsfeld, *J. Aerosol Med.*, 2006, **19**, 372–384.
31 M. Alvarez, L. Yeo and J. Friend, *Nanotechnology*, 2008, **19**, 455103.
32 J. Friend, L. Yeo, D. Arifin and A. Mechler, *Nanotechnology*, 2008, **19**, 145301.
33 P. Barnes, *Curr. Opin. Pharmacol.*, 2001, **1**, 217–222.
34 G. Scheuch, M. J. Kohlhaeufl, P. Brand and R. Siekmeier, *Adv. Drug Delivery Rev.*, 2006, **58**, 996–1008.
35 H. W. Frijlink and A. H. D. Boer, *Expert Opin. Drug Delivery*, 2004, **1**, 67–86.
36 Z. Wang and J. Zhe, *Lab Chip*, 2011, **11**, 1280–1285r.
37 A. Wixforth, C. Strobl, C. G. A. Toegl, J. Scriba and Z. Guttenberg, *Anal. Bioanal. Chem.*, 2004, **379**, 982–991.
38 M. K. Tan, J. R. Friend and L. Y. Yeo, *Lab Chip*, 2007, **7**, 618–625.
39 S. Girardo, M. Cecchini, F. Beltram, R. Cingolani and D. Pisignano, *Lab Chip*, 2008, **8**, 1557–1563.
40 M. Tan, L. Yeo and J. Friend, *EPL*, 2009, **87**, 47003.
41 L. Masini, M. Cecchini, S. Girardo, R. Cingolani, D. Pisignano and F. Beltram, *Lab Chip*, 2010, **10**, 1997–2000.
42 K. Sritharan, C. Strobl, M. Schneider, A. Wixforth and Z. Guttenberg, *Appl. Phys. Lett.*, 2006, **88**, 054102.
43 R. Shilton, M. K. Tan, L. Y. Yeo and J. R. Friend, *J. Appl. Phys.*, 2008, **104**, 014910.
44 M. K. Tan, J. R. Friend and L. Y. Yeo, *Phys. Rev. Lett.*, 2009, **103**, 024501.
45 H. Li, J. Friend and L. Yeo, *Biomed. Microdevices*, 2007, **28**, 4098–4104.
46 K. Kulkarni, J. Friend, L. Yeo and P. Perlmutter, *Lab Chip*, 2009, **9**, 754–755.
47 K. P. Kulkarni, S. H. Ramarathinam, J. Friend, L. Yeo, A. W. Purcell and P. Perlmutter, *Lab Chip*, 2010, **10**, 1518–1520.
48 A. Renaudin, V. Chabot, E. Grondin, V. Aimez and P. G. Charette, *Lab Chip*, 2010, **10**, 111–115.
49 S. Heron, R. Wilson, S. Shaffer, D. Goodlett and J. Cooper, *Anal. Chem.*, 2010, **82**, 3985–3989.
50 J. Ho, M. K. Tan, D. B. Go, L. Y. Yeo, J. R. Friend and H.-C. Chang, *Anal. Chem.*, 2011, **83**, 3260–3266.
51 R. P. Hodgson, M. Tan, L. Yeo and J. Friend, *Appl. Phys. Lett.*, 2009, **94**, 024102.
52 R. Wilson, J. Reboud, Y. Bourquin, S. L. Neale, Y. Zhang and J. M. Cooper, *Lab Chip*, 2011, **11**, 323–328.
53 H. Li, J. Friend, L. Yeo, A. Dasvarma and K. Traianedes, *Biomicrofluidics*, 2009, **3**, 034102.
54 Y. K. Lentz, T. J. Anchordoquy and C. S. Lengsfeld, *J. Pharm. Sci.*, 2006, **95**, 607–619.
55 E. Kleemann, L. A. Dailey, H. G. Abdelhady, T. Gessler, T. Schmehl, C. J. Roberts, M. C. Davies, W. Seeger and T. Kissel, *J. Controlled Release*, 2004, **100**, 437–450.
56 D. Catanese, J. Fogg, D. Schrock, B. Gilbert and L. Zechiedrich, *Gene Ther.*, 2011, **19**, 94–100.